

# Feedback Control Modeling of Plasma Position and Current During Intense Heating in ISX-B

L. A. CHARLTON, D. W. SWAIN, AND G. H. NEILSON

**Abstract**—The ISX-B tokamak at ORNL is designed to have 1.8 MW (and eventually 3 MW) of neutral beam power injected to heat the plasma. This power may raise the  $\beta$  of the plasma to over 5 percent in less than 50 ms, if the plasma is MHD stable. The results of a numerical simulation of the feedback control system and poloidal coil power supplies necessary to control the resulting noncircular (D-shaped or elliptical) plasma are presented. The resulting feedback control system is shown to be straightforward, although nonlinear voltage-current dependence is assumed in the power supplies. The required power supplied to the poloidal coils in order to contain the plasma under the high heating rates is estimated.

## I. INTRODUCTION

THE ISX-B tokamak is designed to study the limits on  $\beta$  attainable in a tokamak subjected to large amounts of supplementary heating. Assuming a constant energy confinement time  $\tau_E$ , and noting that  $\beta = P_{OH} \tau_E / U_p \approx 0.005-0.1$  in most ohmically heated tokamaks to date, then attaining  $\beta = 0.05-0.1$  will require supplemental heating that will provide  $P_{SUPP} = 5-10 \times P_{OH}$ .

In the case of ISX-B, this heating will be provided by two neutral injectors capable of providing up to 1.8 MW at 45 keV into the plasma, with the capability of upgrading the injectors to 3 MW. This power is in the range of 5-10 times the ohmic heating power observed on ISX-A and expected on ISX-B. The resulting sudden changes in plasma pressure caused by such massive heating will require a good feedback control system to keep both plasma position and current at desired values. In this paper, we describe such a simulation that was carried out for the particular case of ISX-B. However, the method and some conclusions are sufficiently general to warrant a more general interest.

There are two special items that were considered for ISX-B, and may be of interest. First, the plasma elongation and shape can be changed by special shaping poloidal coils. This shaping makes the plasma position dynamically unstable in the vertical direction and so an active feedback control system must be used to maintain plasma vertical position. The interaction of this system with the horizontal control system during shaping and/or heating was studied to determine if any instabilities would develop due to cross-coupling. None were found in our system.

Manuscript received March 29, 1979; revised July 20, 1979. This work operated by the Union Carbide Corporation under Contract W-7405-eng-26 with the U.S. Department of Energy.

L. A. Charlton is with the Computer Sciences Division, Oak Ridge National Laboratory, Oak Ridge, TN 37830.

D. W. Swain and G. H. Neilson are with the Fusion Energy Division, Oak Ridge National Laboratory, Oak Ridge, TN 37830.

Second, the ISX-B device is designed to use a coupled control system, where plasma position and current are both strongly affected by current in each of two poloidal coil sets (the "inner" and "outer" windings). That is, the standard ohmic heating and vertical field windings conventionally used in tokamaks have been replaced by two windings with non-orthogonal control functions. This procedure simplified the coil design for ISX-B, and the feedback simulation indicates that the coupled system works effectively at position and current control. Other work, similar to ours, is discussed in [1].

Sections II-IV describe the circuit model, power supply models, and feedback system. Results and conclusions of the simulations are presented in Section V.

## II. CIRCUIT MODEL

A tokamak device as a whole is predominately an electrical system consisting of power supplies, coil sets, eddy currents, etc. It thus seems reasonable to model the behavior of such a system by treating the various components as electrical circuits. Probably the weakest point in our *circuit model* is the assumption that the plasma is a current filament. A real plasma, of course, has a finite extent. Each part of the plasma interacts with the rest of the system in a different way. However, for many purposes, the average behavior of the plasma should be well approximated by a filamentary current located at the mean position of the plasma current, defined by

$$R_1 = \frac{\int_A j(R, z) R dR dz}{\int_A j(R, z) dR dz}.$$

The ISX-B device is a tokamak with a major radius of 93 cm. The vacuum vessel is rectangular with coils mounted around the outside. These coils may be connected in various ways to achieve maximum plasma control. The particular arrangement used in this study is shown in Fig. 1. The inner (*I*) and outer (*O*) coil set currents were used to control the plasma horizontal position and plasma current. Vertical position was maintained by the radial field (*RF*) coil set current. Plasma shape could be changed by varying the current in the set labeled *S*.

The ISX-B vacuum vessel has a liner with a thick wall in which eddy currents can flow. It is split into two halves with insulators, so no net current can flow toroidally in the vacuum vessel. Higher modes, however, can occur, and have a significant effect on the plasma control. We have included the two most significant in this simulation, which we call the first symmetric (in *Z*) and first antisymmetric modes.

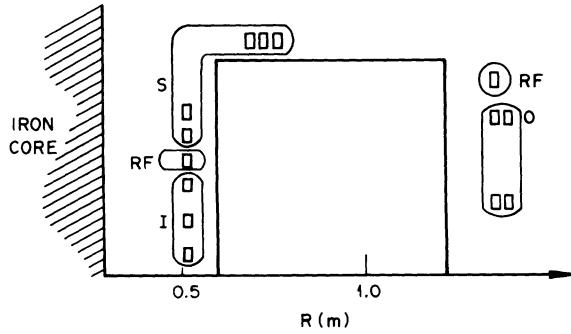


Fig. 1. The chosen coil arrangement. Each rectangle represents a single coil. Only the upper half plane is shown. However, the coils are symmetric about the  $R$  axis.

They have decay times of 5–6 ms, and influence the plasma horizontal and vertical position control, respectively.

The plasma motion was defined by assuming the plasma moves through a series of equilibrium states. The plasma always moves in such a way as to experience a net force of zero. These equilibrium states were described by the formalism of [2] where the horizontal position of the plasma is given by

$$R = -\frac{I_1}{k_1 B_v} (2.1 + \beta_p) \quad (\text{II-1})$$

with poloidal beta ( $\beta_p$ ) given by

$$\beta_p = \frac{k_2 \bar{\beta}}{I_1^2} \quad (\text{II-2})$$

$$k_1 = (4\pi/\mu_o) \sqrt{(1 + \epsilon^2)/2} \quad (\text{II-3})$$

$$k_2 = (q_o R_o/a)^2 2I_1^0/(1 + \epsilon^2). \quad (\text{II-4})$$

$I_1$  refers to the plasma current,  $q_o$  is the safety factor,  $a$  is the effective plasma radius,  $\epsilon$  the elongation,  $\bar{\beta}$  the total average beta, and  $I_1^0(R_o)$  the initial current (position). In (II-1),  $B_v$  is the vertical magnetic field of the plasma “filament” location, given by

$$B_v = \sum_i I_i f_i(R, z) \quad (\text{II-5})$$

where the sum runs over all the current carrying components and the  $f_i$  give the magnetic field per unit current due to each component. The inclusion of the elongation in the above is due to Uckan [3]. The vertical plasma position was defined by requiring that the radial magnetic field  $B_r$  at the plasma location be zero at each instant; i.e.,

$$B_r = \sum_i I_i g_i(R, z) = 0. \quad (\text{II-6})$$

Equations (II-5) and (II-6) assume the magnetic field depends linearly on each current. For the results to be presented later, the  $f_i$  and  $g_i$  were calculated by Tucker and Peng [4] using a two-dimensional code that included the effects of the iron core used in ISX-B.

Equations (II-1)–(II-6) define a plasma equilibrium in a necessarily simple way. The validity of these equations was tested by comparing the currents required for equilibrium to those required when the full Grad-Shafranov equation is solved. The currents at all values of  $\beta$  were the same within

10 percent [5]; for the low- $\beta$  cases agreement was much better.

The current filament model for the plasma was also tested by comparing the currents required for equilibrium using a filament to those needed when the current density was a Gaussian and the magnetic field was given by

$$B_r(R, z) \propto \sum_i \int_{S'} j(R', z') g_i(R', z') I_i \quad (\text{II-7})$$

where  $S'$  is the plasma two-dimensional surface. The currents were the same within 1 percent [6]. The above tests are not claimed to be conclusive. They do, however, tend to justify the model.

With the above, nine equations are defined. They are (see Table I for definition of the subscripts)

$$\sum_j L_{1j} \dot{I}_j + \sum_j I_j \dot{L}_{1j} + R_1 I_1 = 0 \quad (\text{II-8})$$

$$\sum_j L_{ij} \dot{I}_j + I_1 \dot{L}_{i1} + R_i I_i = V_i, \quad i = 2, \dots, 7 \quad (\text{II-9})$$

$$\dot{R} = A + \sum_{i=1}^7 h_i \dot{I}_i + D \dot{Z} \quad (\text{II-10})$$

and

$$\dot{Z} = \sum_{i=1}^7 k_i \dot{I}_i + E \dot{R} \quad (\text{II-11})$$

where the dot over a quantity denotes time derivative, the  $R_i$  are circuit resistances, the  $L_{ij}$  are inductances, and the  $V_i$  are voltages. In the results presented later, the plasma resistance ( $R_1$ ) is taken to be zero and  $V_1 = V_6 = V_7 = 0$ . Equations (II-10) and (II-11) result from taking time derivatives of (II-1) and (II-6). Thus the coefficients in (II-10) and (II-11) are defined and given in Appendix A. Only the  $\dot{L}_{1j}$  enter since all components are stationary except the plasma. These are found from

$$\dot{L}_{1j} = \frac{\partial L_{1j}}{\partial R} \dot{R} + \frac{\partial L_{1j}}{\partial Z} \dot{Z}. \quad (\text{II-12})$$

These nine equations can be written in the form

$$\mathbf{L} \dot{\mathbf{I}} + \mathbf{R} \mathbf{I} = \mathbf{V} \quad (\text{II-13})$$

where the boldface denotes a matrix,

$$\mathbf{L} = \begin{pmatrix} L_{11} & L_{12} & \cdots & L_{17} & \sum_{i=1}^7 I_i \frac{\partial L_{1i}}{\partial R} & \sum_{i=1}^7 I_i \frac{\partial L_{1i}}{\partial Z} \\ L_{21} & L_{22} & \cdots & L_{27} & I_1 \frac{\partial L_{21}}{\partial R} & I_1 \frac{\partial L_{21}}{\partial Z} \\ \vdots & \vdots & & \vdots & \vdots & \vdots \\ L_{71} & L_{72} & & L_{77} & I_1 \frac{\partial L_{71}}{\partial R} & I_1 \frac{\partial L_{71}}{\partial Z} \\ -h_1 & -h_2 & & -h_7 & 1 & -D \\ -k_1 & -k_2 & & -k_7 & -E & 1 \end{pmatrix} \quad (\text{II-14})$$

$$\dot{I} = \begin{pmatrix} \dot{I}_1 \\ \dot{I}_2 \\ \vdots \\ \dot{I}_7 \\ \dot{R} \\ \dot{Z} \end{pmatrix} \quad (II-15)$$

$$R = \begin{pmatrix} R_1 & 0 & 0 & \cdots & 0 & 0 & 0 \\ 0 & R_2 & 0 & & & & \\ 0 & 0 & R_3 & & & & \\ \vdots & \vdots & & \ddots & & & \\ \vdots & \vdots & & & R_7 & 0 & 0 \\ & & & & 0 & 0 & 0 \\ 0 & 0 & \cdots & 0 & 0 & 0 & 0 \end{pmatrix} \quad (II-16)$$

$$V = \begin{pmatrix} 0 \\ V_2 \\ V_3 \\ V_4 \\ V_5 \\ 0 \\ 0 \\ A \\ 0 \end{pmatrix} \quad (II-17)$$

The manner in which the voltages ( $V_i$ 's) were found will be discussed in the next section. Equation (II-13) can be solved for the time derivatives to yield

$$\dot{I} = L^{-1} V - L^{-1} R I. \quad (II-18)$$

This is the form required for standard computer codes which solve differential equations. For the work here, ODE [7] was used.

The radial position of the plasma ( $R$  in (II-10)) must be interpreted as the average radial position of the plasma current density. This, in general, is not the location of the geometrical center of the plasma since the peak in the current density tends to move outward relative to the geometrical center as  $\bar{\beta}$  increases [8]. Thus a method for converting the  $R$  in the preceding equations to a plasma position. The method used here was to parameterize results taken from [8] by the expression

$$\frac{R - R_p}{a} = 0.05 + 0.95 \frac{e^q}{e^q + e^{-q}} \quad (II-19)$$

where

$$q = (\bar{\beta} - 5.8)/2.5 \quad (II-20)$$

$\bar{\beta}$  is expressed in percent,  $a$  is the plasma radius, and  $R_p$  is the plasma position.

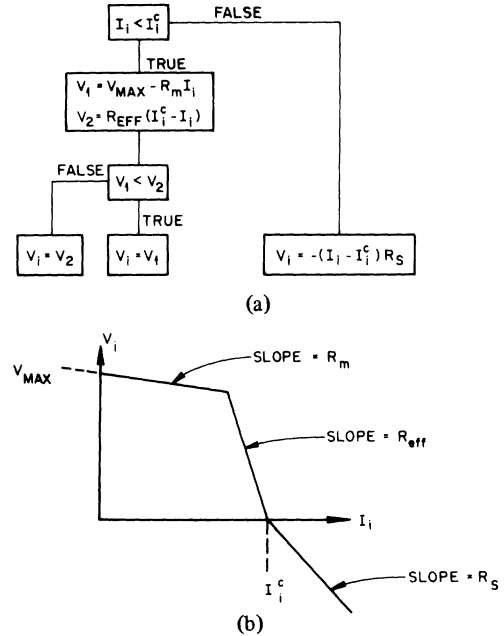


Fig. 2. The behavior of the voltage and current in the current controlled power supply model. A complete explanation is contained in the text.

TABLE I

Label	System Component
1	Plasma
2	Inner coils ( $I$ )
3	Outer coils ( $O$ )
4	Shaping coils ( $S$ )
5	Radial field coils ( $RF$ )
6	Linear 1st antisymmetric mode
7	Linear 1st symmetric mode

### III. POWER SUPPLY MODELS

In the model various parameters can be controlled by changing the voltages (the  $V_i$  of Section II) across the power supplies. If the physical power supply is directly voltage controlled then a reasonable mathematical model is

$$\tau_i \dot{V}_i = e_i \quad (III-1)$$

where  $\tau_i$  is the appropriate time constant and  $e_i$  is the error signal. The error signal, at some time, is the desired amount the voltage should change; this change arriving about  $\tau_i$  later. The specific form for  $e_i$  will be discussed in the next section. This model was used for the shaping coil power supply.

The rest of the power supplies are current controlled and thus a more complicated model is needed. The one used here utilizes a control signal ( $I_i^c$ ) which satisfies

$$\tau_i \dot{I}_i^c = e_i \quad (III-2)$$

where  $\tau_i$  and  $e_i$  are as above. The voltages are then determined by the "logic diagram" shown in Fig. 2(a). The various parameters are chosen to as closely match the model to the behavior of the physical power supply as possible. The model is shown graphically in Fig. 2(b). Plotted is the voltage ( $V_i$ ) as a function of the current ( $I_i$ ). The power supplies for the inner and

TABLE II

	Inner	Outer
$V_{\max}$	72 V	130 V
$R_m$	2 m $\Omega$	0
$R_{\text{eff}}$	$V_r/I_i^c V_r = 1000$ V	56 m $\Omega$
$R_s$	0	2.8 m $\Omega$

outer coils were modeled in this way with parameters as shown in Table II.

The radial field power supply was described by a model which is a somewhat simplified version of that just described. Namely,

$$V_s = R_{\text{eff}}(I_s^c - I_s) \quad (\text{III-3})$$

with  $R_{\text{eff}} = 30$  m $\Omega$ . If  $|V_s| > 36$  V, the voltage was clamped at  $\pm 36$  V.

#### IV. FEEDBACK SYSTEM

The results of the previous sections were used to design the feedback system for ISX-B. "Design" means simply finding the best form for  $e_i$  in (III-1) and (III-2). The primary requirement was that the plasma position be maintained (i.e.,  $R$  and  $Z$  resulting from the solutions to (II-10) and (II-11) be the desired values).

For a change in  $\bar{\beta}$  from 0.5 to 2 percent in 20 ms, it was found that using error signals proportional to the deviation of the position plus the deviation of the velocity from the desired values worked quite well. However, the plasma current varied by large amounts. It was thus necessary to feedback on the plasma current and its first time derivative also. In particular, the following forms were used:

$$e_2 = k_I^P [\Delta I_p + \tau_I^P \Delta \dot{I}_p] \quad (\text{IV-1})$$

$$e_3 = k_O^R [\Delta R + \tau_O^R \Delta \dot{R}] \quad (\text{IV-2})$$

$$e_4 = k_s^I [\Delta I_s + \tau_s^I \Delta \dot{I}_s] \quad (\text{IV-3})$$

$$e_5 = k_{RF}^Z [\Delta Z + \tau_{RF}^Z \Delta \dot{Z}]. \quad (\text{IV-4})$$

The subscripts on the  $e_i$ 's have the same meaning as previously and are defined in Table I. More descriptive labels have been used on the right-hand side of the equations. The  $k$ 's allow the strength of the signal to be varied, the  $\tau$ 's weight the relative importance of the two terms, and

$$\Delta Q = Q - Q_o. \quad (\text{IV-5})$$

$Q$  in the above is any of the quantities appearing in (IV-1)–(IV-4) which are preceded by  $\Delta$  and  $Q_o$  is the desired value. In all cases, the  $\tau$  were chosen to be 5 ms. Making  $\tau$  larger tends to improve the response of the system. However, taking a derivative of an analog signal ( $I_p$  or  $R_p$ ) introduces some noise into the signal, which can cause trouble in the overall feedback loop. A value of 5 ms for  $\tau$  was chosen as a reasonable compromise between these conflicting goals. All parameters in (IV-1) to (IV-4) are given in Table III. These parameters were used to obtain the results in the next section.

TABLE III

$K_I^P$	$K_O^R$	$K_s^I$	$K_{RF}^Z$
+4.0	+60.0 $\frac{\text{kA}}{\text{m}}$	−1.0	+60.0 $\frac{\text{kA}}{\text{m}}$
$\tau_I^P$	$\tau_O^R$	$\tau_s^I$	$\tau_{RF}^Z$
5 ms	5 ms	5 ms	5 ms

As reflected in the equations above, the inner coils were used to control the plasma current, the outer to control the plasma radial position, and the radial field coils were used to control the vertical position. The error signal for the shaping coils (IV-3) was used both to give the plasma the desired shape and to maintain that shape.

The above represents the orthogonal feedback system in that only one quantity is controlled with each coil set. Non-orthogonal systems were used but none were found which gave appreciably better control.

The orthogonal system also has an advantage in that no *locking* of the system can occur. This problem occurred when the inner and outer coils were each used to control both the radial position and the plasma current. For certain situations (raising  $\bar{\beta}$  from 0.5 to 2 percent in 20 ms, for instance), the inner power supply would clamp at zero and the error signal for the outer would be zero due to the radial position demand being equal and opposite to the plasma current demand. Although neither the radial position nor the plasma current had the desired value, the system was receiving a null error signal. It is thus claimed (if all other things are equal) that an orthogonal system should be used. The above together with Sections II and III define what was used for the results to be presented in the next section.

#### V. RESULTS

Studies were done which simulated plasma heating (changes in  $\bar{\beta}$ ), moving the plasma position, changing the plasma current, and shaping the plasma. The control achieved for the first three cases is shown in Table IV. In the table  $\Delta R_{mx}(\Delta I_{mx})$  gives the maximum deviation of the horizontal position (plasma current) from the desired value. In these cases the vertical deviation was zero. Control better than that shown in the table could be achieved if extremely large error signal coefficients (the  $k$ 's in (IV-1) to (IV-4)) were used. For instance, changing  $k_O^R$  to 24000 kA/m reduced  $\Delta R_{mx}$  to less than 1 cm for the heating simulation which changed  $\bar{\beta}$  from 0.5 to 2 percent. The electronics in the actual ISX-B device, however, probably could not handle such large error signal coefficients. Thus the more realistic values given in Table III were used for these results.

For the  $\bar{\beta}$  excursions the control is shown in Figs. 3–5. The plasma position curves show both the plasma location and that of the model current element (the relation between the two is given by (II-19)). All currents except those in the radial field and shaping coils are shown. Control for the  $\bar{\beta} = 1$  percent excursion is unremarkable and is shown only for com-

TABLE IV

Case	$\Delta R_{mx}$ (cm)	$\Delta I_{mx}$ (kA)
$\bar{\beta} = 0.5$ to 1 percent in 20 ms	1	4
$\bar{\beta} = 0.5$ to 2 percent in 20 ms	4	13
$\bar{\beta} = 0.5$ to 5 percent in 50 ms	5	22
$R$ out 3 cm in 15 ms	—	0
$R$ in 3 cm in 10 ms	—	6
$I_p + 10$ kA in 20 ms	0	—
$I_p - 10$ kA in 10 ms	1	—

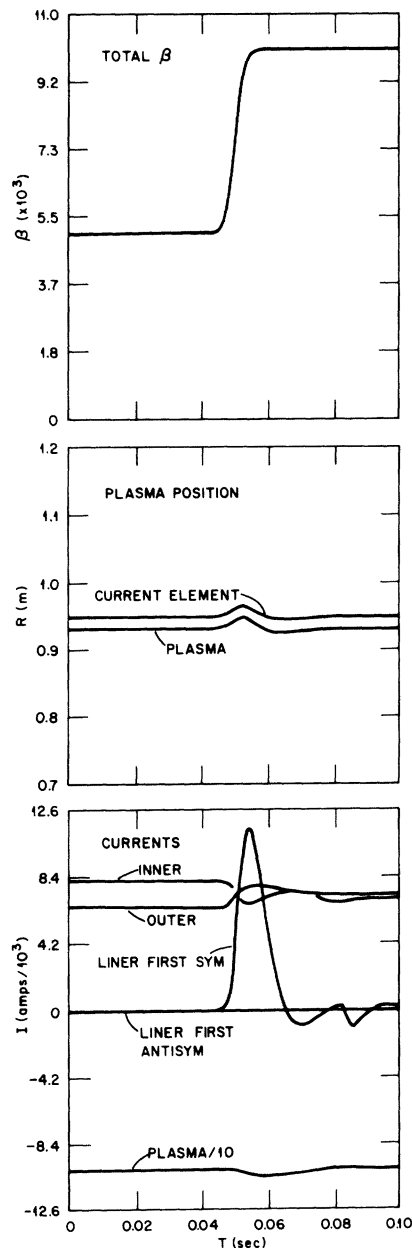


Fig. 3. The horizontal position and current behavior when  $\bar{\beta}$  is raised from 0.5 to 1 percent in 20 ms. Heating starts at 40 ms.

parison. The  $\bar{\beta} = 2$  percent case shows an overshoot in position. That is, the plasma position moves past the desired location. It is, however, back at its initial position about 10 ms after the heating is completed. For  $\bar{\beta} = 5$  percent, there is also an overshoot, but again the desired position is achieved about 10 ms after the heating is stopped.

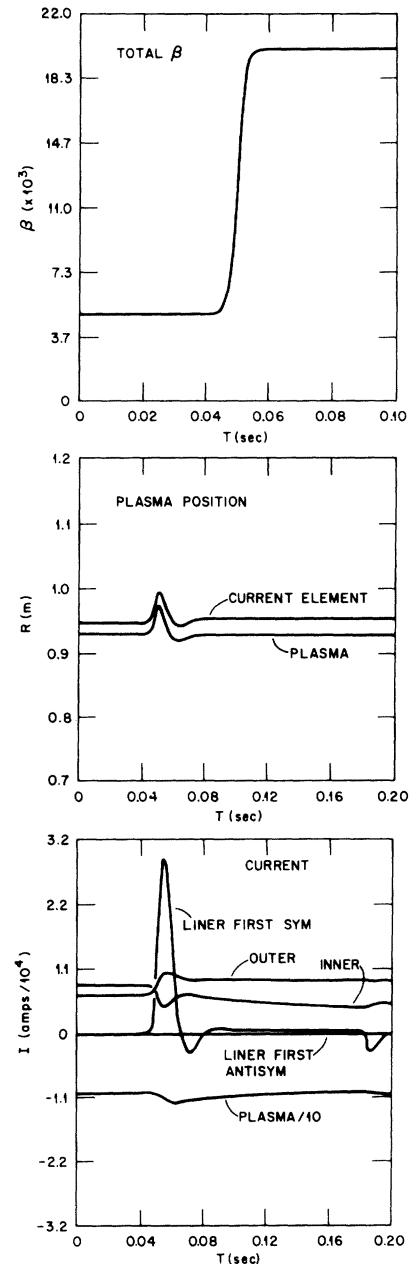


Fig. 4. The horizontal position and current behavior when  $\bar{\beta}$  is raised from 0.5 to 2 percent.

As stated previously, the main purpose of the work presented in this paper was to develop and test a control system which would maintain the desired plasma parameters (position and current) during intense heating. However, a further test of the control system is to demand that the plasma position or current change by some specified amount and find the reaction of the system. For effective control it is also necessary that the parameter that is held constant must remain so. A step function demand that the plasma position move in or out 3 cm was accomplished in 10 ms with a change in the plasma current of less than 1 percent. A step function demand that  $|I_p|$  change by 10 kA was also completed in 10 ms with no significant change in plasma position.

Shaping of the plasma was simulated by requiring that the same amount of current flow in the shaping coils as was required to produce a given elongation in the equilibrium cal-

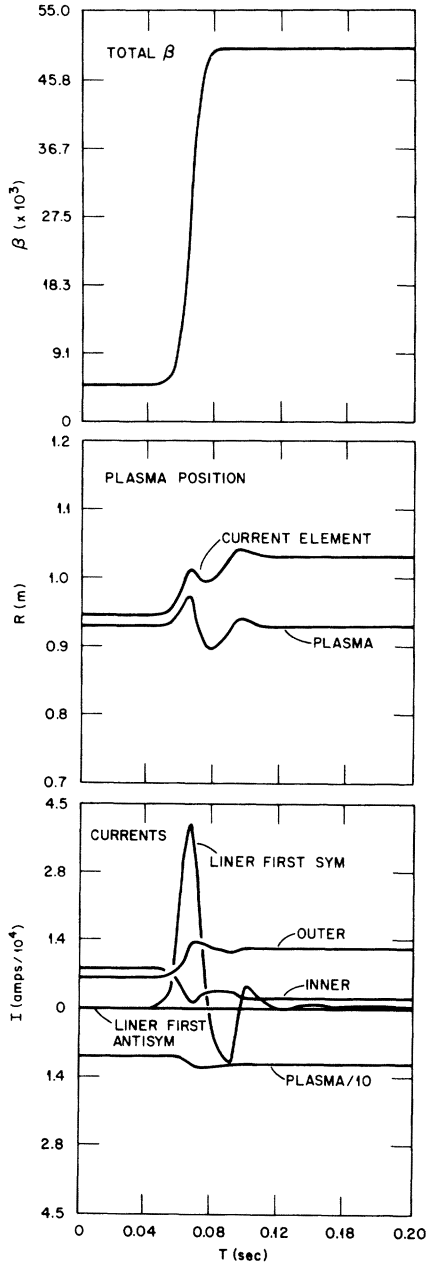


Fig. 5. The horizontal position and current behavior when  $\bar{\beta}$  is raised from 0.5 to 5 percent in 50 ms.

culation of Strickler and Peng [9]. The required currents are given in Table V for two different values of  $\bar{\beta}$ . The vertical instability was studied by initiating a command that the plasma move upward 3 cm in 20 ms and then shutting the vertical feedback system off after 5 ms (i.e., setting  $k_{RF}^z$  in (IV-4) equal to zero). An exponential of the form  $e^{\gamma t}$  was then fitted to the resulting motion giving a growth rate  $\gamma$ . Fig. 6 shows the growth rate as a function of the elongation for the two values of  $\bar{\beta}$ . The plasma is more unstable at small  $\bar{\beta}$  than large and more unstable the larger the elongation. The  $\bar{\beta}$  dependence of the growth rate is due to equilibrium requirements. The smaller  $\bar{\beta}$  is, the larger the amount of current required in the inner coil set relative to the current in the outer coil set. Both the inner and outer coil sets are destabilizing (that is the radial field they produce tends to drive the plasma away from the midplane) but the inner coils

TABLE V

$I_s$ (kA)	$\bar{\beta} = .25\%$					
	+5.0	+3.5	+2.5	+1.5	-.55	-1.1
$\epsilon$	1.10	1.15	1.20	1.27	1.55	1.74
$I_s$ (kA)	$\bar{\beta} = 2.8\%$					
	+1.5	0.	-2.0	-2.5		
$\epsilon$	1.20	1.27	1.55	1.74		

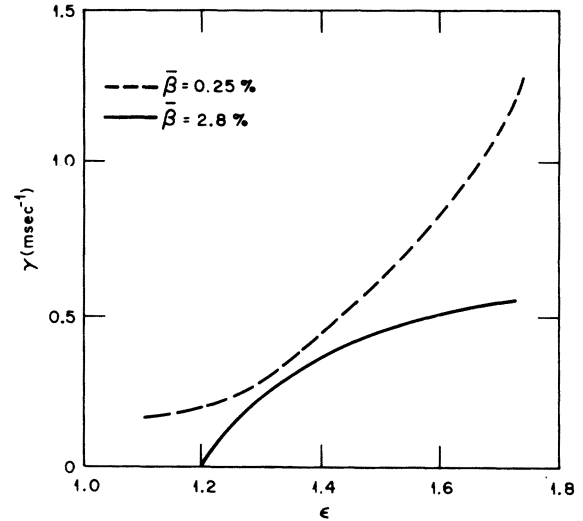


Fig. 6. The growth rate for vertical motion versus elongation for two different values of  $\bar{\beta}$ .

are more destabilizing than the outer. Thus the more current that flows in the inner coils relative to the outer coils the more unstable the plasma is. The dependence of the growth rate on the elongation is due to the destabilizing radial field from the shaping coils. The larger the current in the shaping coils the larger the destabilizing radial field. When the feedback system was left on the largest instability (at  $\bar{\beta} = 0.25$  percent and  $\epsilon = 1.74$ ) was controlled. That is, the command described above was successfully executed.

## VI. CONCLUSIONS

The ISX-B device with the coil arrangement shown in Fig. 1 can control the plasma for a variety of parameter changes with a feedback system which acts only on the plasma current and position and on the first time derivative of these quantities. The "variety of parameter changes" include 1)  $\bar{\beta}$  changes at a 0.075 percent/ms rate, 2) position changes of 3 cm, and 3) plasma current changes of 10 kA. A more general conclusion is that axisymmetric modes can be controlled with a reasonably simple feedback system.

## APPENDIX A

The coefficients appearing in (II-10) are

$$A = \frac{-k_2 \dot{\bar{\beta}} C^{-1}}{k_1 B_v I_1} \quad (\text{A-1})$$

$$B = \frac{-k_2}{k_1 B_v} C^{-1} \quad (\text{A-2})$$

$$h_1 = B \left\{ \frac{2.1}{k_2} - \frac{\bar{\beta}}{I_1^2} \right\} - \frac{I_1 B}{B_v} \left\{ \frac{2.1}{k_2} + \frac{\bar{\beta}}{I_1^2} \right\} f_1(R, Z) \quad (\text{A-3})$$

$$h_i = \frac{-I_1 B}{B_v} \left\{ \frac{2.1}{k_2} + \frac{\bar{\beta}}{I_1^2} \right\} f_i(R, Z), \quad i \neq 1 \quad (\text{A-4})$$

$$D = \frac{-I_1 B}{B_v} \left\{ \frac{2.1}{k_2} + \frac{\bar{\beta}}{I_1^2} \right\} \sum_{i=1}^7 \frac{\partial f_i(R, Z)}{\partial Z} I_i \quad (\text{A-5})$$

$$C = 1 - \left[ \frac{k_2 I_1}{k_1 B_v^2} \right] \left[ \frac{2.1}{k_2} + \frac{\bar{\beta}}{I_1^2} \right] \sum_{i=1}^7 I_i \frac{\partial f_i(R, Z)}{\partial R} \quad (\text{A-6})$$

$$k_i = -\frac{g_i(R, Z)}{F} \quad (\text{A-7})$$

$$E = -\sum_{i=1}^7 I_i \frac{\partial g_i(R, Z)/\partial R}{F} \quad (\text{A-8})$$

$$F = \sum_{i=1}^7 I_i \frac{\partial g_i(R, Z)}{\partial Z}. \quad (\text{A-9})$$

Quantities in the above not given here are defined in the text.

#### REFERENCES

- [1] J. Hugill and A. Gibson, *Nucl. Fusion*, vol. 14, p. 611, 1974; J. L. Anderson *et al.*, *Nucl. Fusion*, p. 629, 1976; J. Fujita *et al.*, in *Proc. 6th Int. Conf. Plasma Physics and Contr. Fusion*, Berchtesgaden, Germany, 1976, IAEA-CN-35/D3, vol. 11, p. 95.
- [2] V. S. Mukovatov and V. D. Shafranov, *Nucl. Fusion*, vol. 11, p. 605, 1971.
- [3] N. Uckan, private communication.
- [4] We wish to thank T. C. Tucker and Y-K. M. Peng for these results.
- [5] We thank D. J. Strickler and Y-K. M. Peng for providing the Grad-Shafranov results.
- [6] We wish to thank R. J. Colchin who suggested this test.
- [7] L. F. Shampine and M. K. Gordon, *Computer Solution of Ordinary Differential Equations: The Initial Value Problem*. San Francisco, CA: Freeman.
- [8] R. A. Dory and Y-K. M. Peng, *Nucl. Fusion*, vol. 21, 1978.
- [9] We wish to thank D. J. Strickler and Y-K. M. Peng for providing the results.

## Numerical Calculations of Magnetoacoustic Oscillations in Toroidal Plasmas

A. L. MCCARTHY

**Abstract**—Magnetoacoustic oscillations in toroidal argon and hydrogen plasmas have been calculated numerically and compared with those in cylindrical plasmas. The toroidal plasmas show reduced enhancement at resonance and shifted resonant frequencies. The position of maximum enhancement of the oscillation fields at resonance which occurs on the minor axis of a large aspect ratio torus is displaced not only toward lower static  $B$  field values but also in a direction at right angles to  $\nabla|B|$  when the aspect ratio is small. As the frequency is increased to values, only moderately higher than resonance, the spatial distribution of the oscillation fields rapidly becomes more complicated than those for the cylindrical plasmas.

### I. INTRODUCTION

**R**ADIAL magnetoacoustic oscillations of axisymmetric magnetized cylindrical afterglow plasmas are sensitive to the radial distribution of both charged and neutral plasma particle densities and to spatial distribution of temperature. Brennan, Jessup, and Jones [1], [2] have reported that the distribution of oscillating magnetic field is very sensitive to

the radial distributions of particle number density and temperature. Further they report that in fitting magnetic flux  $\phi(t)$  measured at different frequencies with a loop external to the plasma, by the integrals of the magnetic fields calculated for chosen profiles, good information on the distribution of the plasma parameters can be obtained when the profiles are adjusted to provide the best fit to the data.

Much of the interest in diagnostic techniques which such reported investigations afford is concerned with methods useful in toroidal geometry. This note reports on numerical calculations of magnetoacoustic oscillation fields in a torus. The calculations have been made only for fully ionized plasmas of uniform number density and temperature in order to gauge the magnitude of the effects which toroidal geometry will have on the oscillation fields in comparison with the cylindrical case. Calculations are made for argon plasmas in which toroidal aspect ratios are 5:1, 11:1, and 12 500 000:1, the exceptionally large aspect ratio representing the cylindrical plasma which can then be treated in exactly the same way as the tori of lower aspect ratio. Further calculations are presented for hydrogen plasmas.

For these calculations the boundary condition on the excitation has been chosen to represent a RF sheet current in the poloidal direction over the whole of the toroidal surface.

Manuscript received September 22, 1978; revised August 24, 1979. This work was supported by grants from the Australian Institute of Nuclear Science and Engineering and the Australian Research Grants Committee.

The author is with the School of Physical Sciences, The Flinders University of South Australia, Bedford Park, S.A., Australia 5042.